Application of curvature of residual operational deflection shape (R-ODS) for multiple-crack detection in structures

Erfan Asnaashari[a] and Jyoti K. Sinha[*]

Dynamics Laboratory, School of Mechanical, Aerospace and Civil Engineering, University of Manchester, Sackville Street, Manchester M13 9PL, UK

Abstract. Detection of fatigue cracks at an early stage of their development is important in structural health monitoring. The breathing of cracks in a structure generates higher harmonic components of the exciting frequency in the frequency spectrum. Previously, the residual operational deflection shape (R-ODS) method was successfully applied to beams with a single crack. The method is based on the ODSs at the exciting frequency and its higher harmonic components which consider both amplitude and phase information of responses to map the deflection pattern of structures. Although the R-ODS method shows the location of a single crack clearly, its identification for the location of multiple cracks in a structure is not always obvious. Therefore, an improvement to the R-ODS method is presented here to make the identification process distinct for the beams with multiple cracks. Numerical and experimental examples are utilised to investigate the effectiveness of the improved method.

Keywords: multiple-crack detection; crack breathing; dynamic characterisation; frequency spectrum; operational deflection shape

1. Introduction

Initiation and propagation of fatigue cracks are very common in structures subjected to cyclic stresses, most of which are below the ultimate tensile stress. Therefore, it is essential to detect fatigue cracks at an early stage of their development to prevent structural failures. The presence of cracks changes the physical properties and consequently vibration behaviour of structures. This feature of cracks has encouraged many researchers to employ vibration-based methods in identifying and locating cracks in different types of structures. A comprehensive overview of various vibration based methods for damage detection in structures can be found in Doebling *et al.* (1996), Wang and Chan (2009), Wei and Pizhong (2011), Yan *et al.* (2007).

External excitation of a structure with fatigue cracks generates non-linear vibration responses along the structure. The non-linear responses are due to repetitive opening and closing (breathing) of the fatigue crack during every cycle of loading. Peng *et al.* (2007) used non-linear output frequency response functions (NOFRFs) to detect breathing cracks in beams based on frequency

---

*Corresponding author, Ph.D. , E-mail: jyoti.sinha@manchester.ac.uk
[a] Ph.D. Student, E-mail: erfan.asnaashari@postgrad.manchester.ac.uk

domain information. The method was sufficiently sensitive to identify the presence of cracks provided that the external excitation with appropriate intensity had been employed. Blunt and Keller (2006) developed planet carrier and planet separation methods based on changes to the modulation of the fundamental gear mesh vibration due to the crack for the purpose of fatigue crack detection in a UH-60A planet gear carrier. They used vibration measurements of healthy and cracked transmissions in test-cell and on-aircraft conditions but only the results for test-cell condition were satisfactory. Bouboulas and Anifantis (2011) constructed the finite element model of a cracked cantilever beam to investigate its vibration behaviour. The breathing of the crack was modelled by defining frictional contact between the surfaces of the crack. They applied fast Fourier transform (FFT) and continuous wavelet transform (CWT) to vibration responses obtained from the finite element model and concluded that both methods can be used for crack detection. Andreaus and Baragatti (2009) investigated the free vibration of healthy and cracked cantilever beams to identify the presence of damage. They first carried out a three-point bending test on aluminium and steel beams to create fatigue cracks. The beams were then excited by an impact hammer to compare the natural frequencies of the intact and cracked beams to recognise the existence of cracks. The need to obtain the information of intact structures can be considered the major limitation of their detection method. Razi *et al.* (2011) presented a method based on empirical mode decomposition (EMD) for fatigue crack detection in an aluminium beam. Here again, vibration response of the healthy structure is used along with that of the cracked structure to produce damage indices. These indices have been shown to be sensitive in terms of identifying the presence of damage. Sinha (2009) utilised bi- and tri-higher order coherence to detect fatigue cracks in a cantilever beam. Yan *et al.* (2013) used the difference between natural frequencies of stiffness regions of beams to detect breathing fatigue cracks. Johnson *et al.* (2010) detailed an approach to capture subharmonic responses generated due to non-linearity of fatigue cracks which can be used for the purpose of damage detection.

Breathing of the fatigue crack also generates higher harmonic components (superharmonics) together with the frequency of excitation in the frequency spectrum of vibration responses. These higher harmonics were used by Tsyfansky and Beresnevich (1998) as well as Semperlotti *et al.* (2009) to identify fatigue cracks in geometrically flexible bars and an isotropic rod respectively. Ullah and Sinha (2011) utilised absolute amplitude of higher harmonics to locate centre and off-centre delamination in composite plates. However, their results lacked phase information of responses to construct the true deflection pattern of structures. By considering both amplitude and phase information of vibration responses, the accurate deflection patterns of structures during external excitation can be obtained, which is called operational deflection shape (ODS). This requires taking measurements at multiple locations along the structure. The use of the ODS for damage detection in different types of structures is presented in Pai and Young (2001), Sundaresan *et al.* (1999) and Zhang *et al.* (2013). However, Asnaashari and Sinha (2013, 2014a, b) have shown the limitations of utilising the ODS alone in locating cracks, and they proposed a new term called residual operational deflection shape (R-ODS) for crack detection in beam-like structures. For beams with multiple cracks, the R-ODS method still shows discontinuities at the location of cracks, but these discontinuities are not clear enough for all conditions. Previously, curvature of mode shapes was used by Kim and Stubbs Kim and Stubbs (1995) to develop a damage detection algorithm for structures. They used the developed algorithm to magnify the effect of damage on mode shapes to predict their locations and severities in a plate for which only a single mode was available. Kim *et al.* (2003) also presented an algorithm based on sensitivity of curvature mode shapes to localise and estimate the severity of damage in beam-like structures. Therefore, in order

to have distinct identification of multiple crack locations for any condition, the second derivative or the curvature of the R-ODS is proposed in this paper and applied to numerical and experimental examples.

2. R-ODS method

The effect of crack breathing on vibration responses in the time domain can be noticed through generation of higher harmonic components of exciting frequency in the frequency domain. Fig. 1 shows a typical time domain and frequency spectrum for a cracked beam where the exciting frequency (1x) as well as its higher harmonics (2x, 3x, 4x ...) can be seen. The R-ODS method is based on constructing the ODS at the frequency of excitation and its higher harmonics to map the deflection pattern of the cracked structure. Asnaashari and Sinha (2013) concluded from numerical simulations that in addition to nonlinearity due to the crack breathing, the ODSs at 2x and other higher harmonics contain the effect of the first harmonic component. The R-ODS method removes the effect of the exciting frequency from the ODSs at higher harmonics initially by normalising all the ODSs at 1x and higher harmonics using Eq. (1)

$$(NODS)_{i,m} = \frac{(ODS_k)_{i,m}}{(MODS)_{i,m}}. \qquad i = 1,2,3,4, \ldots \qquad (1)$$

where $(NODS)_{i,m}$ is the normalised ODS at i-th harmonic for mode m. The subscript k refers to the node number, and $(MODS)_{i,m}$ is the maximum value of ODS data at i-th harmonic for mode m.

The residual operational deflection shape $(R - ODS)$ is then defined as the $NODS$ at the p-th harmonic with respect to the first harmonic as expressed in Eq. (2)

$$(R - ODS)_{p,m} = (NODS)_{p,m} - (NODS)_{1,m}. \qquad p = 2,3,4, \ldots \qquad (2)$$

Therefore, when a cracked beam is excited at its first natural frequency and the R-ODS is calculated for 2x data, p and m are equal to 2 and 1 respectively. In this paper acceleration responses are used to construct the ODSs; however, either displacement, velocity or acceleration responses could be utilised.
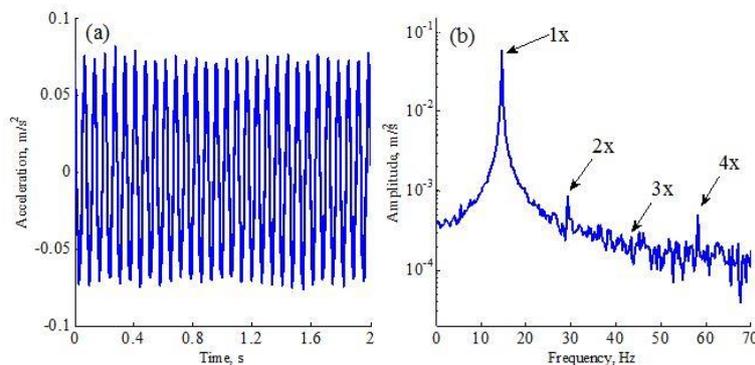

Fig. 1 Calculated acceleration response with noise in (a) time domain and (b) frequency domain for the Fixed-Fixed beam at mode 1

3. Numerical examples

An aluminium beam with cross-section of 25×100 mm^2 and length of 3 m was used. The density and Young's modulus of the beam were 2700 Kg/m^3 and 74 GPa respectively. Multiple cracks with depth of 5 mm were introduced at different locations along both fixed-fixed and simply supported aluminuim beams. Table 1 shows the details of all the investigated beams.

Table 1 Number, locations and dimensions of cracks used in the beams for numerical simulations

Case	B.C.	No. of	Crack Locations [m]	Depth [mm]	Width
Beam 1-N [*]	Fixed-Fixed	2	$X_1=0.5$, $X_2=1.6$	5	0.2
Beam 2-N	Fixed-Fixed	2	$X_1=1.0$, $X_2=2.2$	5	0.2
Beam 3-N	Fixed-Fixed	3	$X_1=0.7$, $X_2=1.2$, $X_3=2.0$	5	0.2
Beam 4-N	Simply supported	2	$X_1=0.8$, $X_2=2.0$	5	0.2
Beam 5-N	Simply supported	2	$X_1=1.2$, $X_2=2.5$	5	0.2
Beam 6-N	Simply supported	3	$X_1=0.4$, $X_2=2.0$, $X_3=2.3$	5	0.2

[*] N refers to numerical beam

Euler-Bernoulli beam elements are employed to model the beam. There are two nodes per element and each node has two degrees of freedom; translational displacement and bending rotation. Proportional damping is obtained using the constructed mass and stiffness matrices.

Various approaches are available to model cracks in beam-like structures (Boltezar *et al.* (1998), Chaudhari and Maiti (2000), Krawczuk and Ostachowicz (1993), Lakshmi Narayana and Jebaraj (1999), Pandey *et al.* (1991), Ratcliffe (1997), Sinha *et al.* (2002)). In this paper, the method proposed in Sinha *et al.* (2002) is used to introduce cracks to the finite element model of the beams. This approach uses the concept of Christides and Barr (1984) to modify the local flexibility in the vicinity of the crack within Euler-Bernoulli beam elements. It assumes that the flexibility from uncracked to cracked section of the beam varies linearly and considers triangular reduction in the stiffness of cracked element. This reduction may happen over more than one element depending upon the crack location. However, the length of each element is modelled to be flexible in such a way that the crack effect remains within a single element.

The breathing of the crack is modelled based on nodal displacements of cracked elements. When the displacement of nodes of the cracked element is greater than zero then the crack is assumed to be open. Otherwise, the crack is considered to be closed. The equation of motion for the cracked beam under external excitation is

$$\mathbf{M}\ddot{\mathbf{y}}(t) + \mathbf{C}\dot{\mathbf{y}}(t) + \mathbf{K}(t)\mathbf{y}(t) = \mathbf{F}(t) \tag{3}$$

where **M**, **C** and **K** are the mass, damping and stiffness matrices for the beam respectively, **y** denotes vertical displacement and **F** is the vector of external force.

In Eq. (3), stiffness matrix is time dependent, because it changes with the opening and closing of the cracks during the external excitation. When the crack is closed, no change happens in the stiffness; therefore, a healthy (global) stiffness matrix can be used in Eq. (3). However, an open crack reduces the stiffness of the cracked element and this reduction needs to be taken into consideration. In the case where multiple cracks exist in the beam (Fig. 2), the number and location of all open cracks at every time step should be determined to consider the stiffness reduction corresponding to each open crack in the global stiffness matrix as follows

$$\mathbf{K}_c = \mathbf{K} - \sum_{p=1}^{n} \Delta\mathbf{K}_{c,p} \tag{4}$$

where $\mathbf{K}_c$ is the stiffness matrix for the cracked beam, $\mathbf{K}$ is the stiffness matrix for the healthy beam (global), n is the number of open cracks and $\Delta\mathbf{K}_{c,p}$ is the reduction in the stiffness due to p-th open crack.

This reduction depends on the location and depth of the crack. The Newmark-β method is used to solve Eq. (3) with time steps of 200 μs assuming that the initial displacement and velocity is zero.

Modal analysis is carried out to compute the natural frequencies of the beams, assuming all the cracks are open (Table 2). Beams are then excited by a sinusoidal input at their first natural frequency. It is quite important to avoid choosing the nodal point(s) of mode shapes as either the crack or excitation location. In order to simulate experimental conditions, a signal to-noise ratio (SNR) of 20 dB is used to pollute the calculated acceleration responses with normalised random noise.

Fast Fourier transform (FFT) was used to convert the time-domain signals into frequency-domain with sampling frequency of 5 KHz. Fig. 1 shows a typical noisy acceleration response from a specific node in time domain and its frequency spectrum for the fixed-fixed beam at mode 1 where the higher harmonics of the exciting frequency can be observed clearly.
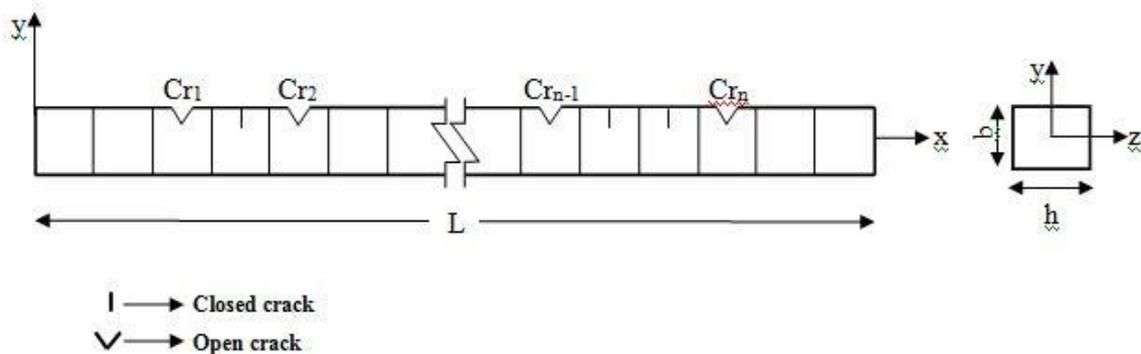

Fig. 2 Schematic view of a beam with multiple open and closed cracks (Cr_1 to Cr_n indicate the number of cracks)

Table 2 The First and second natural frequencies of the numerical beams

Case	Mode 1 [Hz]	Mode 2 [Hz]
Beam 1-N	14.754	40.922
Beam 2-N	14.823	40.382
Beam 3-N	14.757	40.292
Beam 4-N	6.475	25.775
Beam 5-N	6.485	25.957
Beam 6-N	6.482	25.788

4. Curvature of R-ODS

Figs. 3 and 4 depict the numerical R-ODS obtained for the fixed-fixed and simply supported beams with external excitation at the first resonant frequency. Figs. 3, 4(a) and 4(b) show the results for two cracks and Figs. 3 and 4(c) illustrate the R-ODSs when three cracks exist in the beams. It can be observed that the R-ODS figures show discontinuities at the location of cracks. However, these discontinuities are not sufficiently apparent for all the crack locations. For example, although Fig. 3(c) indicates sharp peaks at the location of the second and third cracks, the location of the first crack remains inconspicuous due to its lower amplitude compared to the other two cracks. In fact, the amplitude of discontinuity for most of the crack locations in Figs. 3 and 4 is affected by the curvature of the R-ODSs. Therefore, a better indication for the location of all cracks can be obtained by using the second derivative of the R-ODSs to remove their curvature. The same concept has already been applied to mode shapes, and the second derivative of a beam's mode shape is defined as mode shape curvature (Doebling *et al.* 1998). Pandey *et al.* (1991) analysed a cantilever and a simply supported beam and used finite element analysis to obtain the displacement mode shapes of the two models. Their work demonstrated that changes in the curvature mode shapes were localized in the region of damage, while changes in the displacement mode shapes were not localized and hence could not give any information on the location of the damage. Finally, they confirmed the usefulness of the curvature mode shapes in detecting and locating the state of damage. Lestari *et al.* (2007) developed a method for identifying damage in carbon/epoxy composite beams using curvature mode shapes. They also used a combined analytical and experimental approach to locate the damage through measured curvature mode shapes. The greatest disadvantage of the mode shape curvature method is the difficulty in obtaining the displacement mode shapes experimentally without noise. Because of the noise, the second derivative of the mode shapes may produce many sharp discontinuities which make the crack identification process complicated. Filtering the noise from the mode shapes is an option, but is not practical since the effects of the crack may also be removed. In contrast to mode shape, the R-ODS method uses the difference of the ODSs at the exciting frequency and its higher harmonic which consequently removes the effect of noise from measured responses. As a result, the curvature of the R-ODS is useful for amplifying the effect of cracks and determining their locations.
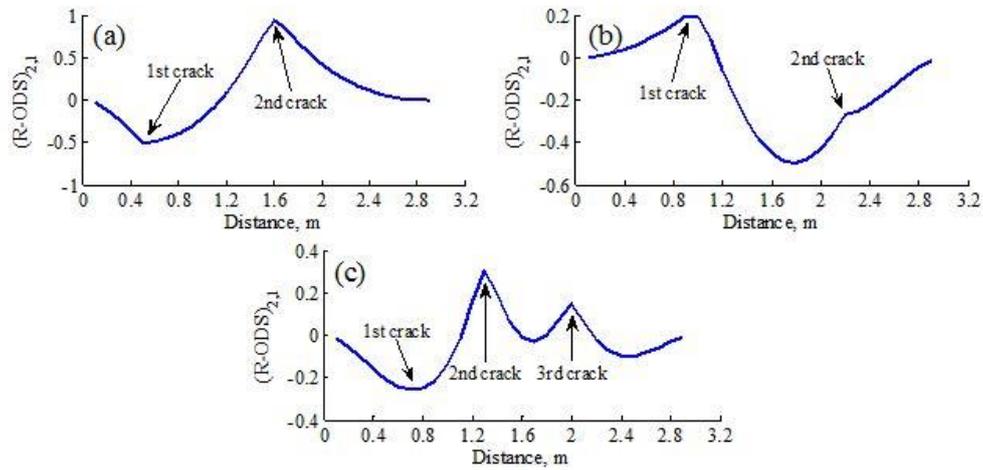
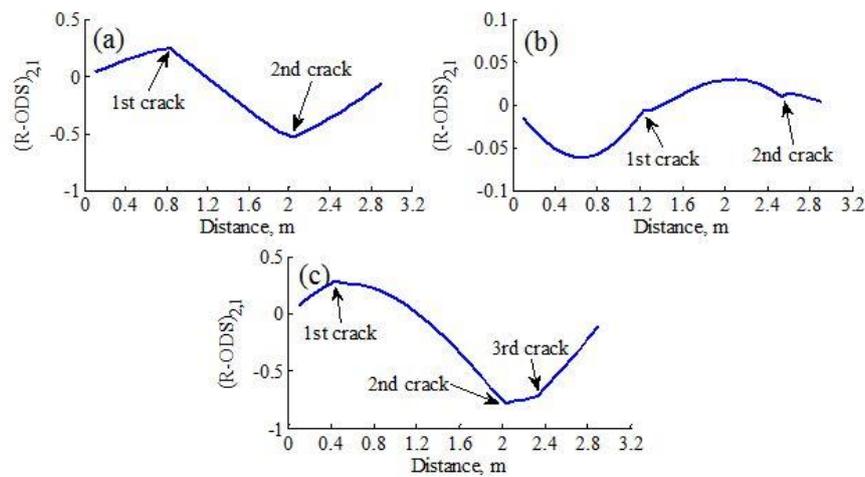Fig. 3 The (R-ODS)$_{2,1}$ results for (a) Beam 1-N, (b) Beam 2-N and (c) Beam 3-N at mode 1

Fig. 4 The (R-ODS)$_{2,1}$ results for (a) Beam 4-N, (b) Beam 5-N and (c) Beam 6-N at mode 1

5. Results and observations

The curvature (second derivative) of the R-ODS results is employed here to investigate its ability to magnify the crack effect. The second derivative can be calculated as

$$d^2(R - ODS_j) = \frac{(R - ODS)_{j+1} - 2(R - ODS)_j + (R - ODS)_{j-1}}{(\Delta x)^2}, \quad j = 2,3, \dots \qquad (5)$$

where j refers to each R-ODS data point and ΔX is the difference between adjacent data points.

Figs. 5 and 6 present the application of the second derivative to the R-ODS results for the fixed-fixed and simply supported beams. As can be seen, the second derivative removes curvature from the R-ODSs and consequently provides a clear indication of the crack locations along the beams. Every single peak in the curvature of R-ODSs for mode 1 represents the location of a crack. According to the numerical simulations, curvature of R-ODS can be used as an accurate method to locate multiple cracks in beams irrespective of their boundary conditions.
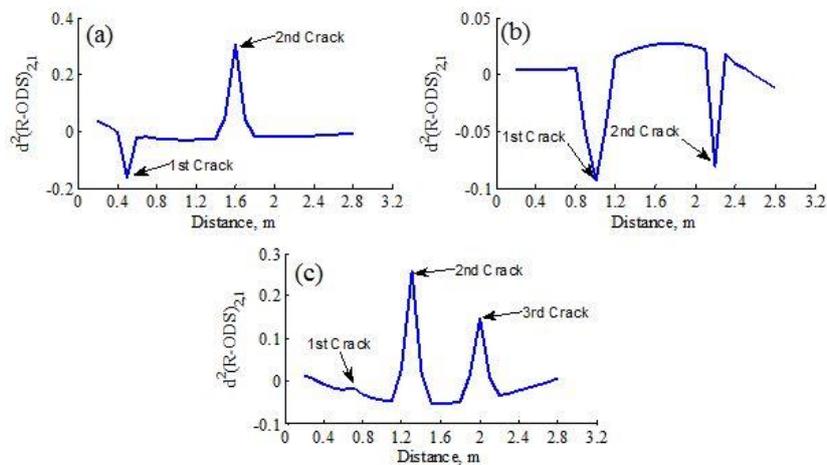

Fig. 5 Curvature of R-ODS for (a) Beam 1-N, (b) Beam 2-N and (c) Beam 3-N at mode 1
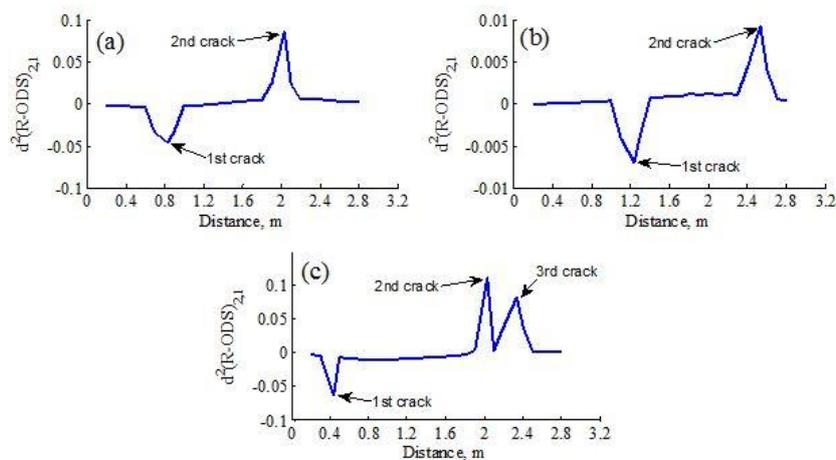

Fig. 6 Curvature of R-ODS for (a) Beam 4-N, (b) Beam 5-N and (c) Beam 6-N at mode 1

6. Experimental examples

Experimental tests were carried out on clamped-clamped and free-free aluminium beams to investigate the reliability of the curvature of R-ODS method. Laser cutting was used to create a single crack in the free-free beam and two cracks in the clamped-clamped beam. Details of the beams and the location of cracks are presented in Table 3. The depth and width of all the cracks are 6 mm and 0.2 mm respectively.

Fig. 7 shows the test setup for the experiments. The complete description for setting up the free-free beam can be found in Asnaashari and Sinha (2014a). Fig. 7(b) depicts the test setup for the clamped-clamped beam where fourteen accelerometers were installed at equal intervals of 19 cm along the beam to acquire vibration responses. The beam was placed on the supports and two U channels were used to clamp the sides and top of both ends in order to represent the fixed-fixed boundary condition to a feasible extent. The excitation force applied by the shaker to the beam was measured using a force gauge. The measured vibration signals were amplified and acquired simultaneously by a 16 bit data acquisition card (Fig. 8) to guarantee valid ODSs with correct magnitude and phase.

Table 3 Specifications of the healthy and cracked beams used in the experiment

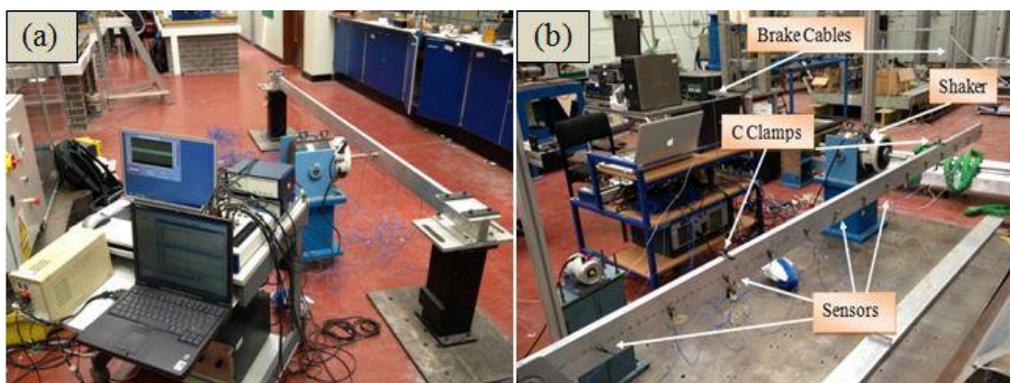| Case	Boundary condition	Length [mm]	Cross-section [mm^2]	No. of crack(s)	Crack location(s) [mm]
Beam 1-E * (Healthy)	clamped-clamped	2550	25×100	--	----
Beam 2-E (Healthy)	Free-Free	3000	25×100	--	----
Beam 3-E	clamped-clamped	2550	25×100	2	$X_1=770$, $X_2=1780$
Beam 4-E	Free-Free	3000	25×100	1	$X_1=1500$

* E refers to experimental beam

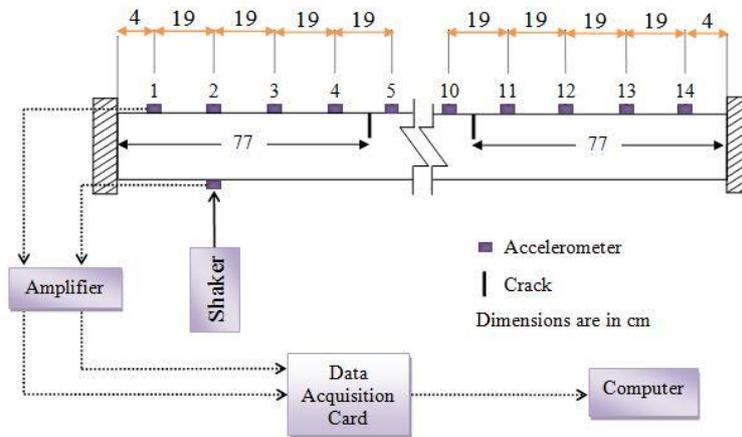Fig. 7 Test setup for (a) Beam 3-E and (b) Beam 4-E (Asnaashari and Sinha 2014a)

Fig. 8 Schematic view of the experiment for the clamped-clamped beam

Modal testing was performed on both healthy and cracked beams in order to obtain the frequency response functions (FRFs). Figs. 9 and 10 present the FRF amplitude and phase for the healthy and cracked clamped-clamped beams. The peak at the frequency of 37.23 Hz in Fig. 9 and that at the frequency of 39.06 Hz in Fig. 10 are related to the second natural frequency of the beams in a vertical direction (perpendicular to the direction of excitation). Table 4 summarises the first three natural frequencies of the beams.

It should be noted that the dimensions of the healthy and cracked beams differ slightly from each other. Also, the location of the clamps and the mounting places of the accelerometers might not be exactly the same in both, which might cause a slightly different mass distribution along each beam. Therefore, inconsistencies can be seen in the results for the second and third natural frequencies.

Table 4 Obtained natural frequencies of the experimental beams

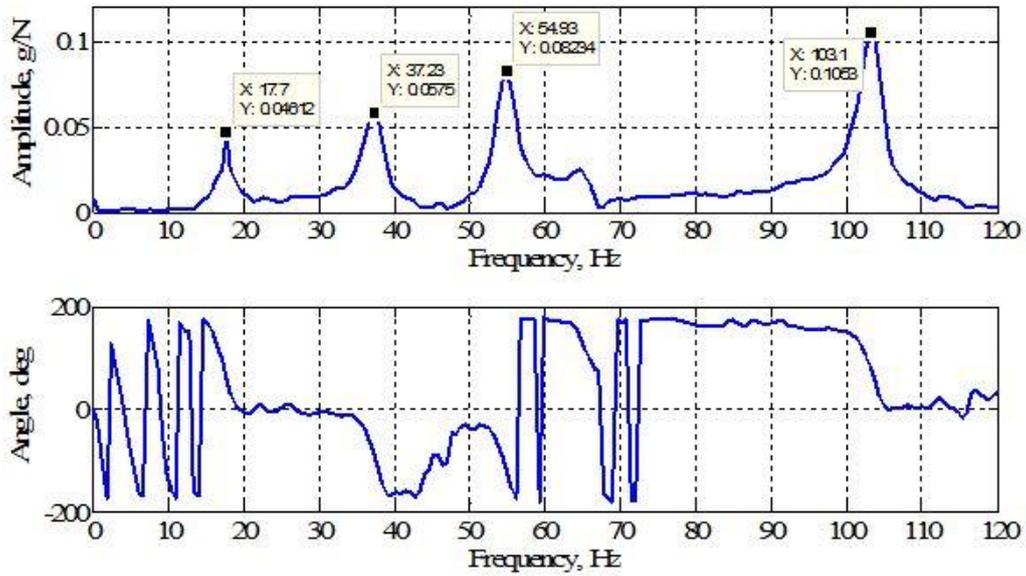| Case	Mode 1 [Hz]	Mode 2 [Hz]	Mode 3 [Hz]
Beam 1-E	17.70	54.93	103.10
Beam 2-E	14.95	39.98	78.43
Beam 3-E	17.09	63.78	105.00
Beam 4-E	14.95	39.98	78.74

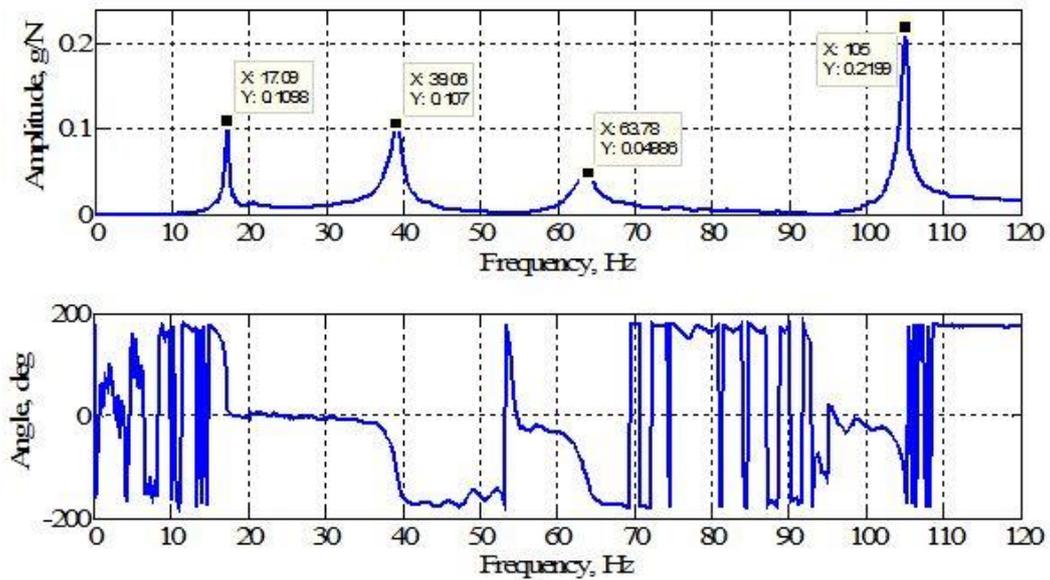Fig. 9 Frequency response function at 80 cm from the right end for Beam 1-E

Fig. 10 Frequency response function at 80 cm from the right end for Beam 3-E
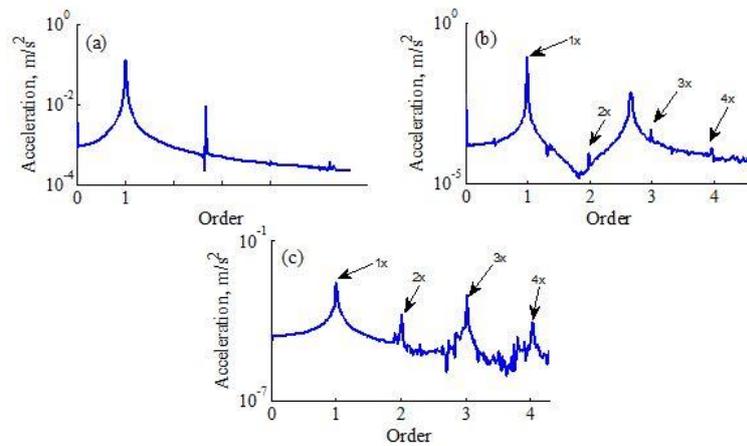
Fig. 11 Ordered frequency spectrum for (a) Beam 2-E, (b) Beam 3-E and (c) Beam 4-E

Based on the FRF results, the aluminium beams were excited by continuous sinusoidal wave at their first natural frequency through the shaker.

Since the R-ODS method is based on the ODSs at higher harmonic components, it is important to make sure that crack breathing has occurred during the experiments. Fig. 11 demonstrates typical ordered frequency spectra for Beams 2-4-E when excited at their first mode. As can be observed, Beam 2-E (healthy) does not show most of the higher harmonic components. However, the spectra for Beam 3-E and 4-E confirm the breathing of crack(s) during external excitation by showing the higher harmonics components clearly.
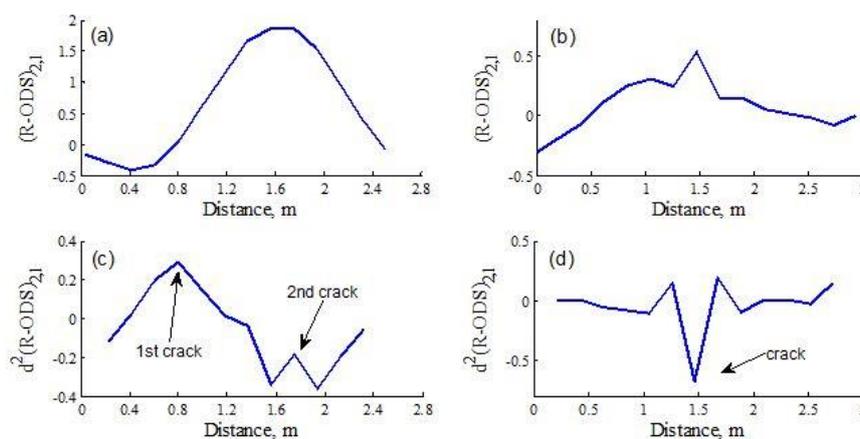

Fig. 12 Experimental R-ODS at mode 1 for Beam 3-E and 4-E (a), (b) and their corresponding d^2R-ODS (c), (d)

Fig. 12 illustrates the experimental R-ODS and its curvature at first mode for the free-free and clamped-clamped aluminium beams. The R-ODS plot for Beam 4-E (Fig. 12(b)) clearly shows the location of the crack. This is due to the fact that the crack is located at the centre of the beam with maximum breathing at the first mode. However, discontinuities related to the crack locations in Beam 3-E are not noticeable in the R-ODS plot (Fig. 12(a)). The better indication of the crack locations in Beam 3-E can be seen in Fig. 12(c) where the second derivative is used to remove the curvature and magnify the discontinuities in the R-ODS plots. The nearest sensors to the crack locations locate the cracks by presenting sharp peaks. The experimental results confirm that the curvature of the R-ODS can be used to detect the location of multiple cracks in beam-like structures.

7. Conclusions

The application of the R-ODS method to beams with multiple cracks is presented. The method utilises the difference between the ODSs at the exciting frequency and its higher harmonics to identify the location of the cracks. The numerical results indicated that in most of the cases, small discontinuities exist in the R-ODS plots at the location of cracks. As a result, the second derivative of the R-ODSs was used to eradicate the curvature and magnify those discontinuities that related to the cracks. Experimental tests were also carried out on free-free and fixed-fixed aluminium beams with single and multiple cracks respectively. It is shown that both the numerical and experimental examples confirm the appropriateness of the curvature of the R-ODS to detect the location of multiple cracks in beam-like structures.

References

Andreaus, U. and Baragatti, P. (2009), "Fatigue crack growth, free vibrations, and breathing crack detection of aluminium alloy and steel beams", *J. Strain Anal. Eng*., **44**(7), 595-608.

Blunt, D.M. and Keller, J.A. (2006), "Detection of a fatigue crack in a UH-60A planet gear carrier using vibration analysis", *Mech. Syst. Signal Pr*., **20**(8), 2095-2111.

Boltezar, M., Strancar, B. and Kuhelj, A. (1998), "Identification of transverse crack location in flexural vibrations of free–free beams", *J. Sound Vib*., **211**(5), 729-734.

Bouboulas, A. and Anifantis, N. (2011), "Finite element modeling of a vibrating beam with a breathing crack: observations on crack detection", *Struct. Health Monit*., **10**(2), 131-145.

Chaudhari, T.D. and Maiti, S.K. (2000), "A study of vibration of geometrically segmented beams with and without crack", *Int. J. Solids Struct*., **37**(5), 761-779.

Christides, S. and Barr, A.D.S. (1984), "One-dimensional theory of cracked Bernoulli-Euler beams", *Int. J. Mech. Sci*., **26**(11-12), 639-648.

Doebling, S.W., Farrar, C.R. and Prime, M.B. (1998), "A summary review of vibration-based damage identification methods", *Shock Vib. Dig*., **30**, 91-105.

Doebling, S.W., Farrar, C.R., Prime, M.B. and Shevitz, D.W. (1996), *RE: Damage Identification and Health Monitoring of Structural and Mechanical Systems from Changes in their Vibration Characteristics: A Literature Review.*

Johnson, D.R., Wang, K.W. and Kim, J.S. (2010), *Investigation of the threshold behavior of subharmonics for damage detection of a structure with a breathing crac*, 765032-765032-9.

Kim, J.T., Ryu, Y.S., Cho, H.M. and Stubbs, N. (2003), "Damage identification in beam-type structures: frequency-based method vs mode-shape-based method", *Eng. Struct.,* **25**(1), 57-67.

Kim, J. and Stubbs, N. (1995), "Model-uncertainty impact and damage-detection accuracy in plate girder", *J. Struct. Eng. - ASCE*, **121**(10), 1409-1417.

Krawczuk, M. and Ostachowicz, W.M. (1993), "Hexahedral finite element with an open crack", *Finite Elem. Anal. Des*., **13**(4), 225-235.

Lakshmi Narayana, K. and Jebaraj, C. (1999), "Sensitivity analysis of local/global modal parameters for identification of a crack in a beam", *J. Sound Vib*., **228**(5), 977-994.

Lestari, W., Qiao, P. and Hanagud, S. (2007), "Curvature mode shape-based damage assessment of carbon/epoxy composite beams ", *J. Intel. Mat. Syst. Str*., **18**(3), 189-208.

Pai, P.F. and Young, L.G. (2001), "Damage detection of beams using operational deflection shapes", *Int. J. Solids Struct*., **38**(18), 3161-3192.

Pandey, A.K., Biswas, M. and Samman, M.M. (1991), "Damage detection from changes in curvature mode shapes", *J. Sound Vib*., **145**(2), 321-332.

Peng, Z.K., Lang, Z.Q. and Billings, S.A. (2007), "Crack detection using nonlinear output frequency response functions", *J. Sound Vib*., **301**(3-5), 777-788.

Ratcliffe, C.P. (1997), "Damage detection using a modified laplacian operator on mode shape data", *J. Sound Vibr*., **204**(3), 505-517.

Razi, P., Esmaeel, R.A. and Taheri, F. (2011), "Application of a robust vibration-based non-destructive method for detection of fatigue cracks in structures", *Smart Mater. Struct*., **20**(11), 115017.

Semperlotti, F., Wang, K.W. and Smith, E.C. (2009), "Localization of a breathing crack using super-harmonic signals due to system nonlinearity", *AIAA J*., **47**(9), 2076-2086.

Sinha, J.K. (2009), "Higher order coherences for fatigue crack detection", *Eng. Struct*., **31**(2), 534-538.

Sinha, J.K., Friswell, M.I. and Edwards, S. (2002), "Simplified models for the location of cracks in beam structures using measured vibration data", *J. Sound Vib*., **251**(1), 13-38.

Sundaresan, M.J., Schulz, M.J., Hill, J., Wheater, E.A., Ferguson, F. and Pai, P.F. (1999), "Damage detection on a wind turbine blade section", *Proceedings of the IMAC XVII Conference.* Orlando, FL.

Tsyfansky, S.L. and Beresnevich, V.I. (1998), "Detection of fatigue cracks in flexible geometrically non-linear bars by vibration monitoring", *J. Sound Vib*., **213**(1), 159-168.

Ullah, I. and Sinha, J. K. (2011), "Experimental vibration study on the healthy and delaminated composite plates", *J. Physics: Conference Series*, **305**(1), 012048.

Wang, L. and Chan, T.H.T. (2009), R*eview of vibration-based damage detection and condition assessment of bridge structures using structural health monitoring*, The Second Infrastructure Theme Postgraduate Conference : Rethinking Sustainable Development: Planning, Engineering, Design and Managing Urban Infrastructure. Queensland University of Technology, Brisbane.

Wei, F. and Pizhong, Q. (2011), "Vibration-based damage identification methods: a review and comparative study", *Struct. Health Monit*., **10**(1), 83-111.

Yan, G., De Stefano, A., Matta, E. and Feng, R. (2013), "A novel approach to detecting breathing-fatigue cracks based on dynamic characteristics", *J. Sound Vib*., **332**(2), 407-422.

Yan, Y.J., Cheng, L., Wu, Z.Y. and Yam, L.H. (2007). "Development in vibration-based structural damage detection technique", *Mech. Syst. Signal Pr*., **21**(5), 2198-2211.

Zhang, Y., Lie, S.T. and Xiang, Z. (2013), "Damage detection method based on operating deflection shape curvature extracted from dynamic response of a passing vehicle", *Mech. Syst. Signal Pr*., **35**(1-2), 238-254.